The Airborne Glacier and Land Ice Surface Topography Interferometer (GLISTIN-A)

Delwyn Moller
James Carswell
Remote Sensing Solutions
Barnstable, Massachusetts, USA
dkmoller@remotesensingsolutions.com

Scott Hensley
Gregory Sadowy
Charles Fisher
Yunling Lou
Jet Propulsion Laboratory,
California Institute of Technology
Pasadena, California, USA

Abstract—This **In May 2009 a new radar technique for mapping ice surface topography was demonstrated in a Greenland campaign as part of the NASA International Polar Year (IPY) activities. The demonstration occurred using the airborne glacier and ice surface topography interferometer (GLISTIN-A): a 35.6 GHz single-pass interferometer implemented as an adaptation to the Jet Propulsion Laboratory (JPL) L-band uninhabited airborne vehicle synthetic aperture radar (UAVSAR). Although the technique of using radar interferometry for mapping terrain has been demonstrated before, this was the first such application at millimeter-wave frequencies. GLISTIN-A performance indicates swath-widths over the ice between 5-7km, with height precisions ranging from 30cm-3m at a posting of 3m x 3m. However, for this application the electromagnetic wave will penetrate an unknown amount into the snow cover thus producing an effective bias that must be calibrated. To evaluate this, GLISTIN-A flew a coordinated collection with the NASA Wallops airborne topographic mapper (ATM) on a transect from Greenland's summit to its West coast. Preliminary comparisons with the ATM lidar altimeter have bounded the effective penetration depth of the Ka-band interferometric phase center to less than 1m over the dry firn. Currently, ESTO has funded the transition of GLISTIN-A to operational status through the AITT program.**

Keywords-interferometery, radar, ice.

I. INTRODUCTION

ESTO's Airborne Innovative Technology Transition (AITT) program recently funded the transition of a swath-based suborbital sensor in support of the Climate Variability and Change Earth Science Focus Area. Initially developed under the NASA International Polar Year activities, a Ka-band interferometric interface to the UAVSAR system [1] was flown to Greenland to demonstrate high-resolution, high-precision ice surface topography mapping capability. Figure 1 shows that configuration as installed on the NASA Gulfstream III. Analysis from that campaign have established the success of the technique and demonstrated that the system performance meets (and exceeds at times) our stated science requirements [2]. This was also the first ever demonstration of single-pass interferometry at millimeter-wave frequencies.

Figure 2 shows a summary of some of the first-processed results, taken over a relatively rugged area along the West coast of Greenland at 69.1°N latitude, 49.7°W longitude (just South of Jakobshavn glacier) from an altitude of 8 km above mean sea level (AMSL). The results shown are for posting of 3m x 3m and report height precisions that vary from 30 cm in the near range to about 3 m in the far range extending up to a 7.5km swath. However to meet the accuracy requirements the systematic measurement and instrument biases must be calibrated. Of these a particular concern is the interferometric penetration of the electromagnetic wave into the snow cover, which is an unknown bias to the surface height measurement. This quantity, while modeled has no supporting measurements and must be quantified for the interferometer to provide scientifically useful data. Section II summarizes a preliminary bounding assessment of the interferometric penetration of the Ka-band signal into the snow cover from IPY data collected at Greenland's Summit.

Called GLISTIN-A (Glacier and Ice Surface Topography Interferometer - Airborne), ESTO has provided funding to transition this to a permanent capability within the UAVSAR program. This transition will incorporate two fundamental, yet low-risk upgrades: 1) a solid state power amplifier (SSPA) will enable unpressurized operation making the Ka-band assembly compatible with UAV operation and potentially enabling access to the Antarctic continent and 2) changing the front-end switch configuration to supporting ping-pong operation. The combination of the SSPA and radar front-end upgrade will enable swaths in excess of 10km at higher operating altitudes (greater than10km above ground level). Section III summarizes the improvements that are underway under the AITT program and the current status of that effort.

II. PRELIMINARY PENETRATION DEPTH ASSESSMENT

The Airborne Terrain Mapper lidar system on a NASA P3 [3] and GLISTIN-A on the Gulfstream III collected data over

The research described in this paper was conducted at Remote Sensing Solutions and Jet Propulsion Laboratory, California Institute of Technology, Pasadena, CA under a contract with National Aeronautics and Space

a calibration site established at NSF's Summit station on 5/4/2009 (GLISTIN-A) and 5/5/2009 (ATM). Staff at Summit deployed and precision surveyed radar corner-reflectors as an absolute height reference in addition to the ATM. The dry firn is considered to be the limiting case for interferometric penetration into the snow cover which produces an effective bias of the radar height measurement for the surface. Figure 3 shows the radar swaths with the ATM lidar tracks overlaid within the orange boxes. Approximately 10,000 ATM points are contained in each scene. The ATM track in the 18° heading data are located in the radar far range where the height noise is about 2-3 m. In the -162° heading data the lidar track is located in the near range where the radar height noise is 20-30 cm. (Note data not fully calibrated so small baseline error results in elevation wiggles on the order of 30 cm.)

The vertical distribution of scatterers within a resolution element causes height biases and decorrelation of interferometric data. Assuming an exponentially attenuating volume $\sigma(z) = \mathrm{e}^{-\eta z}$, (where $\eta = \frac{2\pi \,\mathrm{Im}(\sqrt{\varepsilon})}{\lambda}$, ε is the dielectric constant and λ is the transmitted wavelength) the volumetric decorrelation caused by the vertical distribution of the scatterers over a depth d can be expressed as follows:

$$\gamma_v = \frac{\int \sigma(z) e^{ik_z z}\, dz}{\int \sigma(z)\, dz}$$

$$= \frac{\eta}{\eta - ik_z} \frac{e^{-ik_z h_m}}{\sinh(\frac{\eta d}{2})} \left[\sinh(\frac{\eta d}{2}) \cos(\frac{k_z d}{2}) - i \cosh(\frac{\eta d}{2}) \sin(\frac{k_z d}{2}) \right]$$

where k_z is the vertically projected wavenumber. The penetration phase bias is given by

$$\arg(\gamma_v) = k_z h_m + \tan^{-1}(\frac{k_z}{\eta}) - \tan^{-1}\left(\tan(\frac{k_z d}{2}) \coth(\frac{\eta d}{2}) \right).$$

Using this simplified model (which ignores Mie scattering effects: a more accurate model will be the subject of a subsequent analysis) we predict penetration height biases on the order of 10-30cm. Figure 4 shows histograms of the elevations differences between radar and lidar and consistent with a differential penetration of less than 1m. After calibration is complete we expect to obtain better bounds.

III. AITT Activities

The AITT implementation will incorporate two distinct changes that improve performance and also enable unpressurized and autonomous operation of the Ka-band specific hardware. Table 1 summarizes the modifications. While the peak transmit power is equivalent, the TWTA used during IPY required pressurized operation. Additional advantages of the SSPA is a reduction in front-end losses since it is located in the pod next to the antennas and there is no hard duty cycle limit like that imposed with tube amplifiers. The second performance upgrade is the addition of ping-pong capability which improves the height precision by a factor of two. Reflected in Table 1, with these modifications we can collect data at higher altitudes of operation for increased swath for the same range of incidence angles (near, mid and far swath correspond to look angles of 15°, 31° and 50° respectively). The height precisions quoted indicate an equivalent height performance for GLISTIN-A, but covering a nominal swath of 10km rather than 6km. (Notionally one could also degrade the swath for a higher precision product).

Currently the RF hardware design has been finalized and is in fabrication. An initial thermal and mechanical assessment for the Ka-band implementation has indicated that all the GLISTIN-A specific hardware can be accommodated within the UAVSAR pod. To transition between the L-band UAVSAR and GLISTIN-A will require just the swapping of antenna panels and plugging the air-intake cooling duct. Survival heaters will be placed on the electronics housed within the pod (i.e. no cooling is needed during operation in the air).

IV. Conclusions and Future Work

The success of the IPY Ka-band interferometer proof-of-concept campaign has lead to a continuation through the AITT program which will make GLISTIN-A an operational NASA airborne sensor. Successful engineering and science flights demonstrated height mapping capability with high precision. A key parameter to understand and quantify in order to utilize this data for cryospheric science is the effective interferometric penetration depth of Ka-band electromagnetic wave into the snow cover. Here we presented the bounding estimates over the limiting case – the dry firn. Our analytical prediction is a penetration of 10-30cm, while our initial comparison limits it to less than 1m. This estimate and the model will be refined in ongoing work. Note that for high-resolution coastal and glacial mapping the penetration bias not only becomes less, but it is also less of concern in terms of the science requirements in those regions. It is really on the ice-sheets that this quantity needs to be well characterized in terms of the science requirements.

The AITT program is well into the first year and new hardware is currently under fabrication. The operational GLISTIN-A system will provide enhanced performance over the IPY configuration, with swath-mapping capability increased to over 10km. In addition, operationally the transition between the L-band UAVSAR and GLISTIN-A will be relatively seamless requiring only the swapping of antenna panels since all Ka-band hardware will be self-contained within the panel assembly. Currently first engineering flights of the upgraded and operational GLISTIN-A system are anticipated for Spring of 2012.

Acknowledgment

We would like to acknowledge Thierry Michel, Xiaoqing Wu and Ron Muellerschoen at the Jet Propulsion Laboratory for their contributions to processing the data shown.

REFERENCES

[1] P. A. Rosen, S. Hensley, K. Wheeler, G. Sadowy, T. Miller, S. Shaffer, R. Muellerschoen, C. Jones, H. Zebker, S. Madsen, "UAVSAR: A New NASA Airborne SAR System for Science and Technology Research," *Proc. IEEE Conference on Radar*, 24-27 April 2006, pp8.)

[2] Moller, D.; Hensley, S.; Sadowy, G. A.; Fisher, C. D.; Michel, T.; Zawadzki, M.; Rignot, E.; , "The Glacier and Land Ice Surface Topography Interferometer: An Airborne Proof-of-Concept Demonstration of High-Precision Ka-Band Single-Pass Elevation Mapping," Geoscience and Remote Sensing, IEEE Transactions on , vol.PP, no.99, pp.1-16, 0 doi: 10.1109/TGRS.2010.2057254

[3] W. Krabill, R. Thomas, C. Martin, R. Swift, and E. Frederick, "Accuracy of airborne laser altimetry over the Greenland ice sheet." *International Journal of Remote Sensing* 16 (7) (May): 1211-1222, 1995.

Table 1: Summary of changes from IPY to GLISTIN-A and performance/swath advantage (highlighted)

Parameter	**Unit**		**IPY**	**GLISTIN-A**
Peak transmit power (at antenna)	W		40 (TWTA)	40 (SSPA)
Receive Losses	dB		5	2
Ping-pong			No	Yes
Nominal flight altitude (AGL)	km		7	11
Nominal Swath	km		6	10
Height precision (30x30m posting)	m	15^o	0.06	0.10
		31^o	0.14	0.11
		50^o	0.50	0.49

Figure 1: Picture of NASA Gulfstream III with pod configured for Ka-band interferometry. Lower insert shows close-up with details of the two antennas

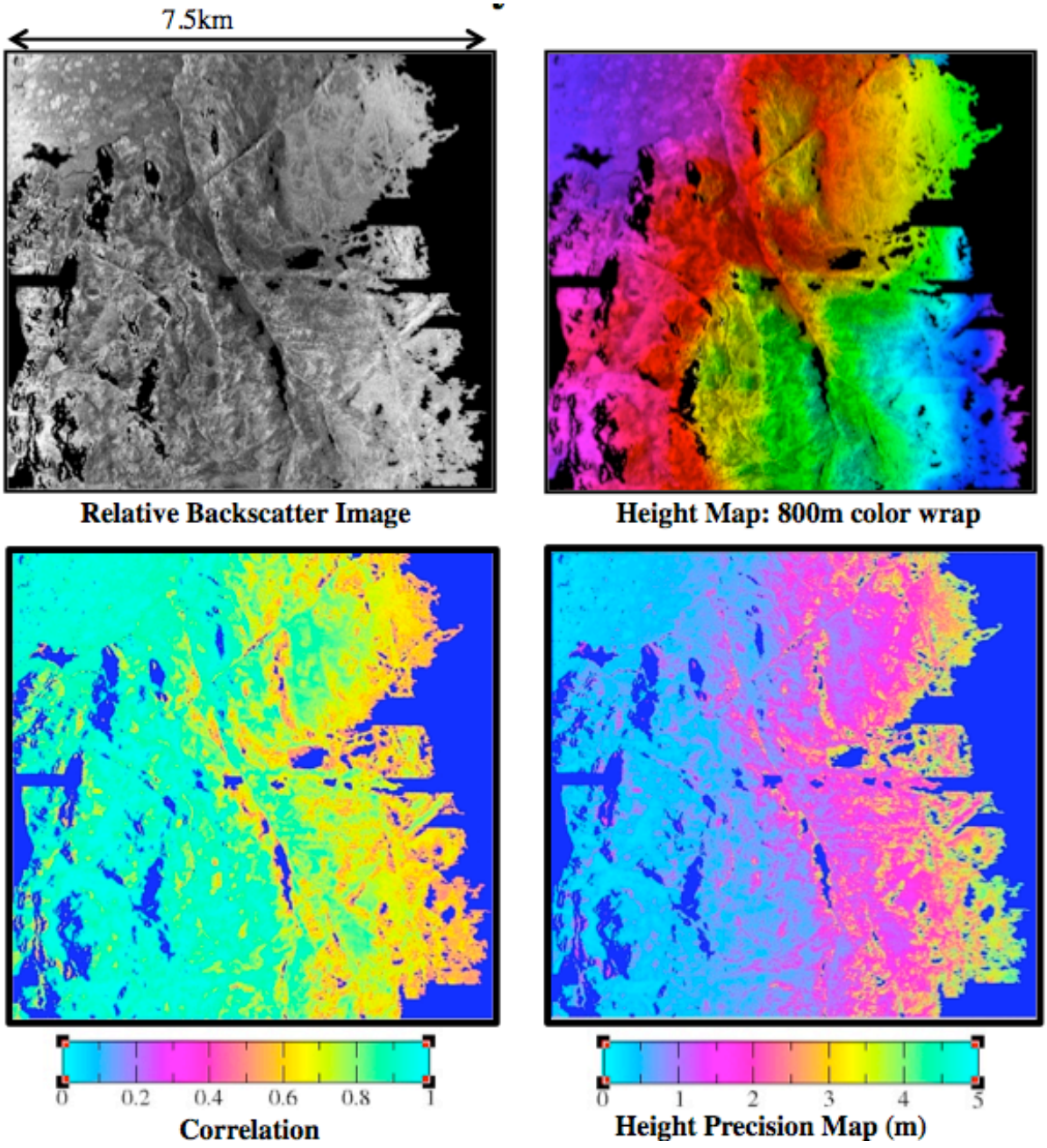

Figure 2: Ka-band maps at 3m x 3m posting generated from data collected on May 1, 2009 near the Greenland coast. a) relative backscatter image and b) Ka-band radar elevation map. Elevation contours are color coded with a wrap of 800 m, i.e. from red to red represents an elevation change of 800 m. c) Interferometric correlation and d) height error map (right) generated from the correlation data. Note the height accuracy varies from 30 cm in the near range to about 3 m in the far range. The data if averaged to the 30 m posting as needed for glacial science application will meet the 50 cm height accuracy requirements almost everywhere in the swath

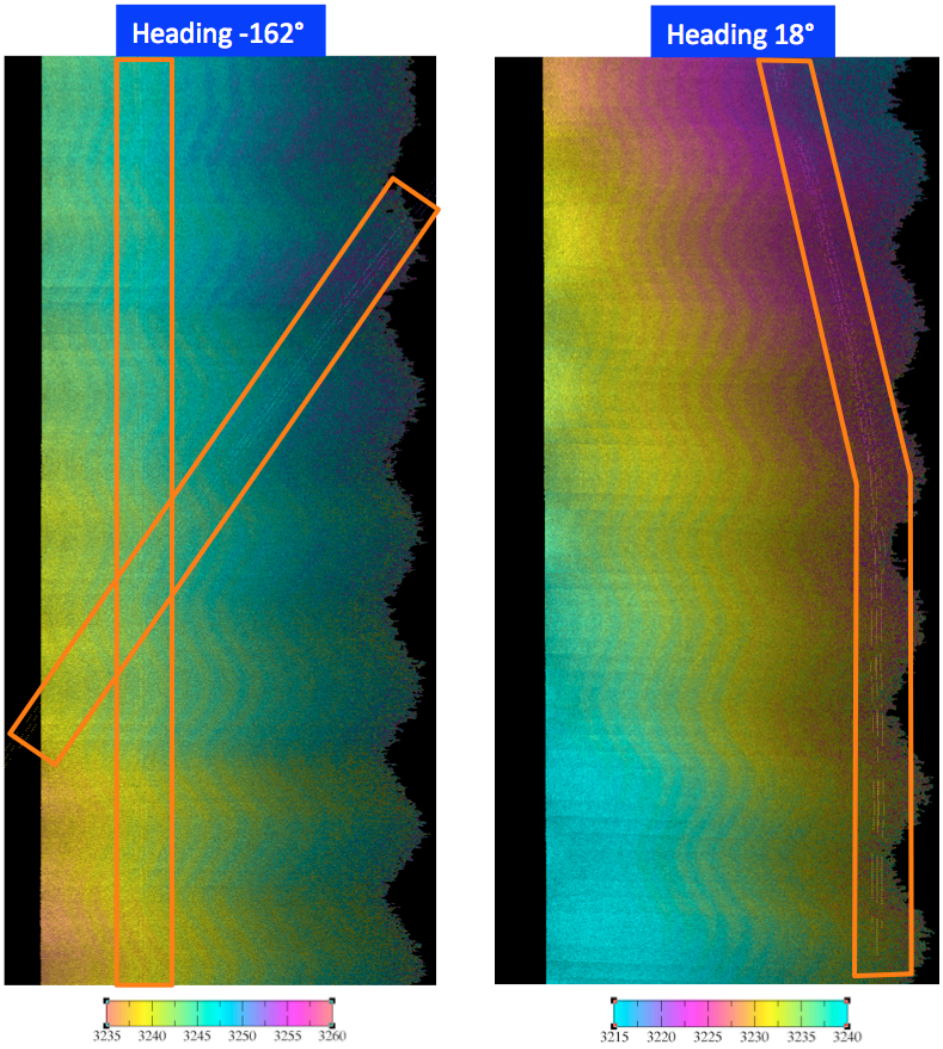

Figure 3: Ka-band maps at 3m x 3m posting generated from data collected on May 4, 2009 at Greenland's Summit. Data from the ATM is superimposed and can be distinguished within the orange boxes**.**

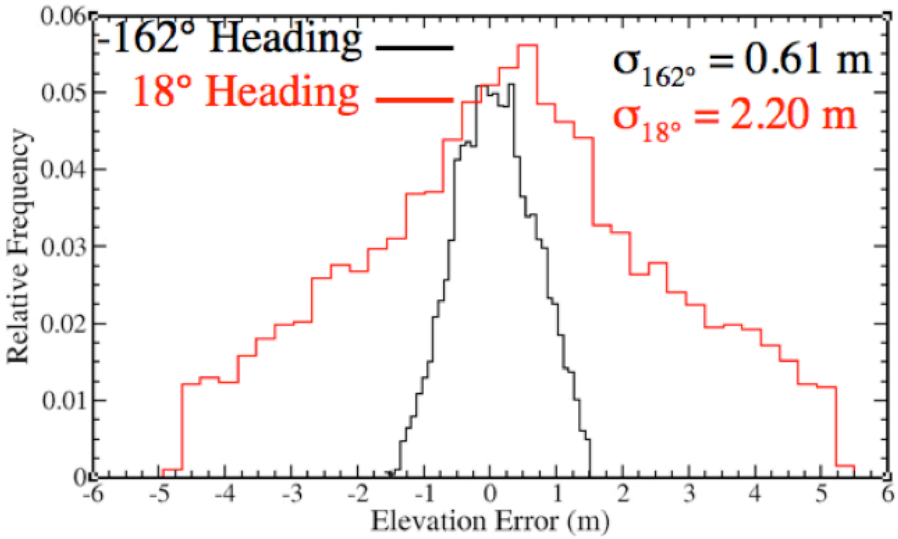

Figure 4: Histograms of the elevations differences between radar and lidar and consistent with a differential penetration of less than 1m